Monte Carlo approach to sequential neutron emission from fission fragments

S. Lemaire,* P. Talou, T. Kawano, M. B. Chadwick, and D. G. Madland

Theoretical Division, Nuclear Physics Group, Los Alamos National Laboratory, Los Alamos, New Mexico, 87545, USA

(Received 15 February 2005; published 5 August 2005)

We have implemented a Monte Carlo simulation of fission fragment statistical decay by sequential neutron emission. Within this approach, we calculate the center-of-mass and laboratory prompt neutron energy spectra as a function of the mass of fission fragments and integrated over the whole mass distribution. We also assess the prompt neutron multiplicity distribution $P(\nu)$, both the average number of emitted neutrons and the average neutron energy as a function of the mass of the fission fragments [respectively $\bar{\nu}(A)$ and $\langle \varepsilon \rangle(A)$]. We investigate the average total energy available for prompt γ-ray emission as a function of the mass of the fission fragments $\bar{E}_\gamma(A)$. We also calculate neutron-neutron correlations such as the full matrix $\bar{\nu}(A, \text{TKE})$ as well as correlations between neutron energies. Two assumptions for partitioning the total available excitation energy among the light and heavy fragments are considered. Results are reported for the neutron-induced fission of ^{235}U (at neutron energy of 0.53 MeV) and for the spontaneous fission of ^{252}Cf.

I. INTRODUCTION

The prompt fission neutron spectrum $N(E)$ plays an important role in various nuclear technologies, both in energy and nonenergy applications. From a more fundamental point of view, an accurate knowledge of $N(E)$ can shed some light on the nuclear fission process itself. The Los Alamos (or Madland-Nix) model [1] has been commonly and successfully used over the years to predict the spectrum and the average number of prompt neutrons, $\bar{\nu}$, as funtions of both the fissioning nucleus and its excitation energy. It simulates the deexcitation of the fission fragments by evaporating neutrons having the Weisskopf spectrum, with an assumption of simple triangular-shaped initial nuclear temperature distribution. However, the Los Alamos model cannot predict more specific physical quantities, such as the prompt neutron multiplicity distribution $P(\nu)$, because it does not follow the neutron evaporation process in detail, but instead averages over the decay chain. The present work is an attempt to go a step beyond the Los Alamos model and look in more detail at the fission fragment decay process.

We extended the Los Alamos model [1] by implementing a Monte Carlo simulation of the statistical decay (Weisskopf-Ewing) of the fission fragments (FF) by sequential neutron emission. To simulate the initial distribution of total excitation energy (TXE) possible in the FF, we use experimental data on the total kinetic energy distributions $P(\text{TKE})$, nuclear masses, neutron separation, and kinetic energies (in the case of neutron induced fission) when available and results from calculations otherwise. To simulate the decay of each fission fragment, one needs to know how the TXE is distributed in the two fragments. Two different hypotheses for partitioning the TXE are considered: (i) both fission fragments have the same nuclear temperature as the fissioning compound nucleus temperature and (ii) the TXE is split according to experimental values of the average total number of emitted neutrons [$\bar{\nu}_{\exp}(A)$], average

center-of-mass neutron energies [$\langle \varepsilon \rangle_{\exp}(A)$], and total average energies removed by γ rays [$\bar{E}_{\exp,\gamma}(A, Z)$] as a function of a fission fragment mass.

The Monte Carlo approach leads to a much more detailed picture of the decay process and various physical quantities can then be assessed: the center-of-mass and laboratory prompt neutron energy spectrum, $\Phi(\varepsilon)$ and $N(E)$ respectively, integrated over the whole FF mass distribution, the same quantities are obtained as a function of the FF mass $N(\varepsilon, A)$, the prompt neutron multiplicity distribution $P(\nu)$, the average number of emitted neutrons as a function of the FF $\bar{\nu}(A, Z, \text{TKE})$ and total kinetic energy (TKE), the average neutron energy as a function of the FF and TKE, $\langle \varepsilon \rangle(A, Z, \text{TKE})$, the total average γ-ray energy $\bar{E}_\gamma(A)$, and all possible neutron-neutron correlations.

This article is organized as follows: the theoretical models and numerical methodology are first introduced, including a short explanation for all input parameters entering in our calculations. The second part is devoted to the presentation and discussion of our numerical results obtained for two fissioning systems: ^{252}Cf (sf) and $n+^{235}$U at $E_n = 0.53$ MeV. A conclusion and outlook completes this article.

II. THEORETICAL APPROACH

A. Methodology

Unlike in the original Los Alamos model where many quantities are lumped together, our approach tries to follow in detail the statistical decay of the FF by sequential emission of individual neutrons. A Monte Carlo approach allows us to follow in detail any reaction chain and to record each event in a history-type file, which basically mimics the results of a real fission process. We assume binary fission and we satisfy baryon number and charge conservation throughout.

1. Mass distribution

We first sample the FF mass and charge distributions, and pick a pair of light and heavy nuclei that will then decay by

emitting zero, one or several neutrons. This decay sequence is governed by neutron emission probabilities at different temperatures of the compound nucleus and by the energies of the emitted neutrons.

The FF mass and charge distributions is

$$Y(A, Z) = Y_{\exp}(A) \, P(Z), \tag{1}$$

where $Y_{\exp}(A)$ represents the experimental preneutron emission FF mass distribution and $P(Z)$ the corresponding charge distribution. We sample over the experimental preneutron emission FF mass distribution $Y_{\exp}(A)$ and pick a pair of light and heavy fission fragments (A_L and A_H respectively). We then sample over the charge distribution $P(Z)$, which is approximately Gaussian:

$$P(Z) = \left(\frac{1}{c\pi}\right) e^{-(Z-Z_p)^2/c}, \tag{2}$$

where Z_p the most probable charge for the light or heavy fragment obtained from a corrected unchanged charge distribution (UCD) assumption because of Unik *et al.* [2], and c is the width parameter defined as follows:

$$c = 2\left(\sigma^2 + \tfrac{1}{12}\right). \tag{3}$$

With σ the average charge dispersion. An experiment of Reisdorf *et al.* [3] on the preneutron emission charge distributions for thermal neutron induced fission of ^{235}U gave $\sigma = 0.4 \pm 0.05$.

For given light, heavy, and compound nucleus mass numbers the most probable charge is given by the following:

$$\left(Z_p^L - \frac{1}{2}\right) \Big/ A_L = \frac{Z_c}{A_c} = \left(Z_p^H + \frac{1}{2}\right) \Big/ A_H, \tag{4}$$

where $c, L,$ and H refer to compound fissioning nucleus, light fission fragment, and heavy fission fragment, respectively.

Of course, the particular decay path followed by this pair of nuclei depends on the available excitation energies, which can be deduced in the following manner.

2. Total FF excitation energy

The total excitation energy TXE possible for the light and heavy pairs (A_L, Z_L) and (A_H, Z_H) are as follows:

$$\mathrm{TXE}(A_L, A_H, Z_L, Z_H) = E_r^*(A_L, A_H, Z_L, Z_H) + B_n(A_c, Z_c)$$
$$+ E_n - \mathrm{TKE}(A_L, A_H), \tag{5}$$

where $E_r^*(A_L, A_H, Z_L, Z_H)$ is the energy release in the fission process, which is given, in the case of binary fission, by the difference between the compound nucleus and the FF masses:

$$E_r^*(A_L, A_H, Z_L, Z_H) = M(A_c, Z_c) - M(A_L, Z_L)$$
$$- M(A_H, Z_H), \tag{6}$$

where M is the mass excess in mega-electron-volts.

In Eq. (5) $B_n(A_c, Z_c)$ and E_n are the separation and kinetic energies of the neutron inducing fission. In the case of spontaneous fission, both $B_n(A_c, Z_c)$ and E_n terms in Eq. (5) are zero.

The total FF kinetic energy in Eq. (5) is labeled TKE(A_L, A_H). In fact, TKE is not a single value but it has a distribution assumed to be Gaussian, whose mean value and width are taken from experimental data. In particular, we perform a Monte Carlo sampling over this distribution to get a total kinetic energy for the selected pair of FF. The distribution is given by the following:

$$P(\mathrm{TKE}) = \frac{1}{\sigma_A \sqrt{2\pi}} \, e^{\frac{-(\mathrm{TKE} - \overline{\mathrm{TKE}}_A)^2}{2\sigma_A^2}}, \tag{7}$$

where $\overline{\mathrm{TKE}}_A$ and σ_A are the mean value and width of total kinetic energy distribution function, respectively.

3. Energy partition

One of the long-standing questions about the nuclear fission process is how does the available total excitation energy get partitioned into the light and heavy fragments. In the present study, we have considered two hypotheses for the partitioning:

(i) Partitioning (H1) so that both light and heavy fragments share the same temperature (hypothesis identical to the one made in the Los Alamos model [1]) at scission. From this condition, it follows that the initial excitation energy of given FF is as follows:

$$E_{L,H}^* = \mathrm{TXE} \frac{1}{1 + \frac{a_{H,L}}{a_{L,H}}}, \tag{8}$$

where L and H refer to the light and heavy system, a is the level density parameter.

(ii) Partitioning (H2) using the experimental $\bar{\nu}_{\exp}(A)$, $\langle\varepsilon\rangle_{\exp}(A)$, and $\bar{E}_{\exp,\gamma}(A)$ to infer the initial excitation of each fragment. This condition reads as follows:

$$E_{L,H}^* = \mathrm{TXE} \frac{\bar{\nu}_{\exp}(A_{L,H})\langle\eta\rangle_{L,H} + \bar{E}_{\exp,\gamma,(L,H)}}{\sum\limits_{i=L,H} [\bar{\nu}_{\exp}(A_i)\langle\eta\rangle_i + \bar{E}_{\exp,\gamma,i}]}, \tag{9}$$

where $\langle\eta\rangle_{L,H}$ is equal to the average energy removed per emitted neutron

$$\langle\eta\rangle_{L,H} = \langle\varepsilon\rangle_{\exp}^{L,H} + \tfrac{1}{2}B_{2n}(A_{L,H}, Z_{L,H}). \tag{10}$$

It is the sum of the average center-of-mass energy of the emitted neutrons for a given FF and, to average over pairing effects, we take the average fission fragment neutron separation energy as one half of the two neutron separation energy for a given initial fission fragment. In Eq. (9), we also take into account the average total energy removed by γ rays $\bar{E}_\gamma(A)$. If we further assume that:

$$\frac{\bar{\nu}_L \langle\eta\rangle_L}{\bar{E}_{\gamma,L}} = \frac{\bar{\nu}_H \langle\eta\rangle_H}{\bar{E}_{\gamma,H}}. \tag{11}$$

then we recover the approximation made by Browne and Dietrich [4], which is not unreasonable based on neutron binding energies systematics. The total average energy removed by γ rays from each FF is given by $\bar{E}_{\exp,\gamma,L}$ for the light one and $\bar{E}_{\exp,\gamma,H}$ for the other.

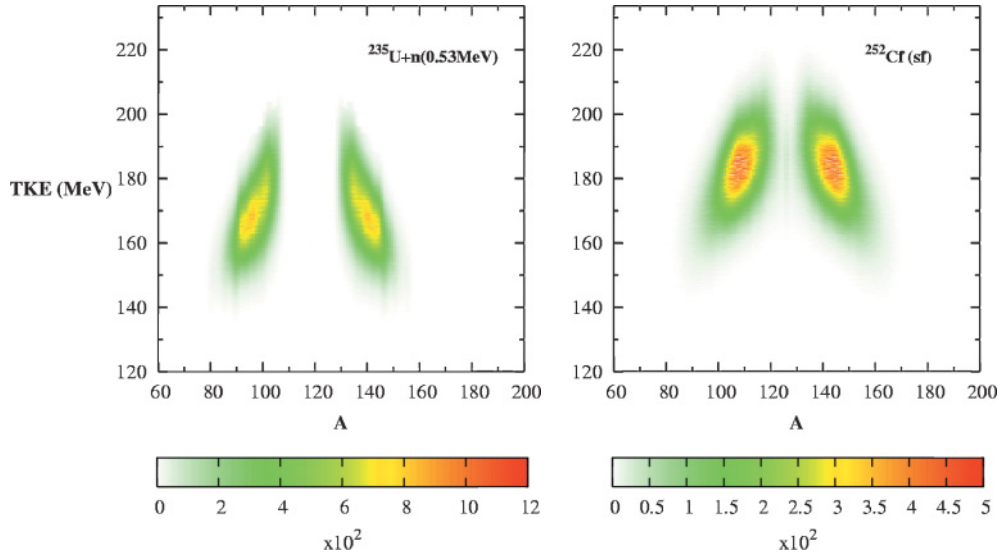FIG. 1. (Color) Experimental yields used in our calculations plotted as a function of the mass number of the FF and TKE for ^{252}Cf(sf) on the right and $n(0.53$ MeV$)+^{235}$U reaction on the left.

4. Neutron evaporation

Within the Fermi gas model, the initial FF excitation energy $E_{L,H}^*$ is simply related to the nuclear temperature $T_{L,H}$. The probability for the FF to emit a neutron at a given kinetic energy is obtained by sampling over the Weisskopf spectrum at this particular temperature [5]. When the energy dependence for the inverse process of compound nucleus formation [$\sigma_c(\varepsilon)$] is taken into account, this spectrum reads as follows:

$$\phi(A, Z, \varepsilon, T) = k(T)\sigma_c(\varepsilon)\varepsilon e^{\frac{-\varepsilon}{T_{A-1,Z}}}, \qquad (12)$$

where $k(T)$ is the normalization constant at a given temperature, $T_{A-1,Z}$ is the nuclear temperature of the residual nucleus given by the following:

$$T_{A-1,Z} = \sqrt{\frac{E^*(A, Z) - B_n}{a_{A-1,Z}}}, \qquad (13)$$

with $a_{A-1,Z}$ the level density parameter of the nucleus.

This temperature corresponds to the temperature of the nucleus diminished by the neutron separation energy of the given nucleus, B_n. In addition, the derivation of Eq. (12) assumes that the energy of the emitted neutrons is small compared to the residual FF excitation energy $E^*(A, Z) - B_n$. When this condition is not satisfied, the probability of emitting a neutron becomes less than what is given by Eq. (12) because of the competition with γ-ray emission. In the particular case of $\varepsilon > E^*(A, Z) - B_n$, the emission of neutrons by a FF is forbidden.

Assuming a constant value for the cross section for the inverse process of compound nucleus formation, $\sigma_c(\varepsilon)$, the normalized spectrum in Eq. (12) becomes:

$$\phi(A, Z, \varepsilon, T) = \frac{\varepsilon}{T_{A-1,Z}^2}e^{\frac{-\varepsilon}{T_{A-1,Z}}}, \qquad (14)$$

where the $T_{A-1,Z}^2$ factor in the denominator arises because of the spectrum normalization.

The neutron emission of energy ε from the FF at the excitation energy E^* produces a residual nucleus with the excitation energy

$$E^*(A - 1, Z) = E^*(A, Z) - \varepsilon - B_n. \qquad (15)$$

The sequential neutron emission ends when the excitation energy of the residual nucleus is less than the sum of its neutron separation energy and pairing energy. By including the pairing energy, we simulate the competition between neutron and γ emission at lower excitation energies. This very crude approximation will be removed later on when properly describing this competition.

The transformation of the center-of-mass spectrum to the laboratory spectrum is done by assuming that neutrons are emitted isotropically in the center-of-mass frame of a FF. So, sampling over the angle of emission of the neutron $\theta_n \in [0, \pi]$ for each nucleus (A, Z), we infer the neutron energy in the laboratory frame, taking into account the recoil energy of the residual nucleus.

B. Input parameters

This section describes the various input parameters that enter in our model calculations, for both the neutron-induced fission of ^{235}U (at 0.53 MeV neutron energy) and for the spontaneous fission of ^{252}Cf.

1. Mass distribution

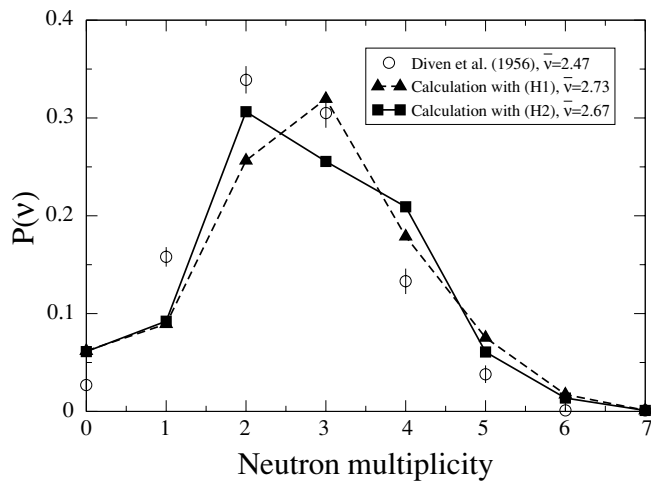The fission mass yields have been measured extensively and precisely for several nuclei and energies. In the present

FIG. 2. Neutron multiplicity distribution for $n(0.53 \text{ MeV}) + ^{235}\text{U}$ reaction. Full square symbols (■) are from our Monte Carlo calculation assuming partitioning of FF total excitation energy as a function of $\bar{\nu}_{exp}(A)$ (H2 hypothesis), triangles (▲) are the result obtained under the assumption of an equal temperature of complementary FF (H1 hypothesis). The points are experimental data from Diven *et al.* [15] at 80-keV incident neutron energy.

calculation, we sample over the preneutron fragments yields $Y_{exp}(A)$, i.e., before neutron evaporation, as reconstructed from the experimentally measured fission products mass distribution. In particular, we use the data by Hambsch [6] for $^{252}\text{Cf(sf)}$, and the data by Schmitt [7] for the thermal neutron-induced fission of ^{235}U (Fig. 1).

In the case of neutron induced $n(0.53 \text{ MeV}) + ^{235}\text{U}$ reaction, 255 fragments were considered to represent the $Y(A, Z)$ of Eq. (1). In particular, we considered 85 equispaced fragment masses (between $76 \leqslant A \leqslant 160$) with three isobars per fragment mass, around the most probable charge Z_p given by Eq. (4).
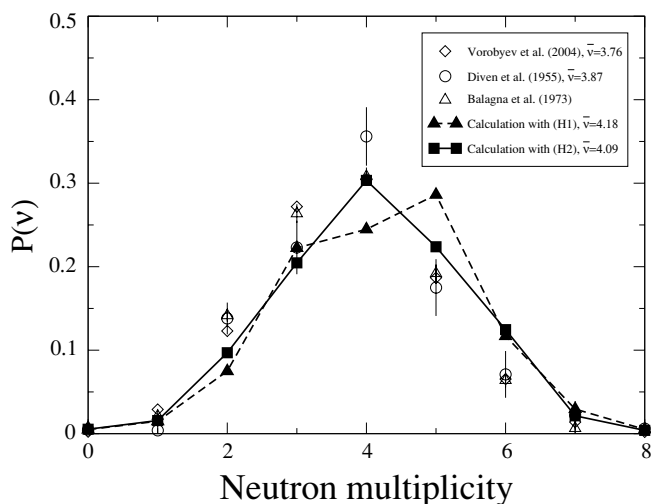

FIG. 3. Neutron multiplicity distribution for $^{252}\text{Cf(sf)}$. The points are experimental data from Refs. [15,17,18].
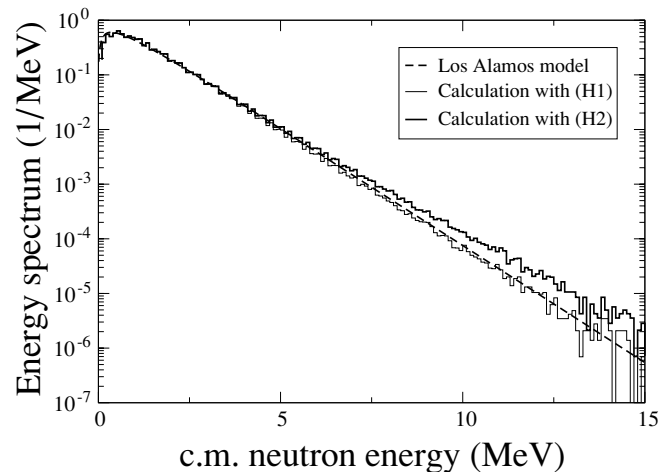

FIG. 4. Neutron energy spectrum in the FF center-of-mass system for $n(0.53 \text{ MeV}) + ^{235}\text{U}$ reaction. The thick line is our Monte Carlo calculation assuming partitioning of FF total excitation energy as a function of $\bar{\nu}_{exp}(A)$ (H2 hypothesis) and the thin line is the result obtained under the assumption of an equal temperature of complementary FF (H1 hypothesis). The dashed line is result of the Los Alamos model calculation using the optical model potential of Becchetti and Greenlees for the inverse process of compound nucleus formation.

In the case of spontaneous fission of ^{252}Cf, we used 315 FF between $74 \leqslant A \leqslant 178$ with 105 equally spaced fragment masses and again three isobars per fragment mass.

2. Nuclear masses

Nuclear masses are used to calculate the energy release for a given pair of FF in Eq. (6). It is a function of both mass and charge number of complementary fragments. The data table by Audi, Wapstra, and Thibault [8] was used in the present calculation.
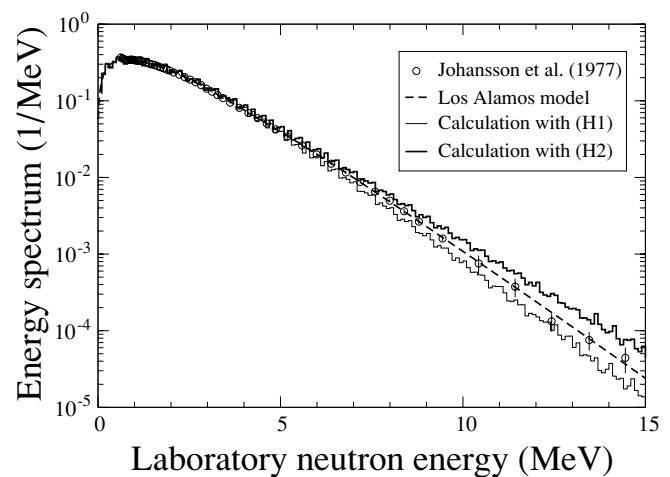

FIG. 5. Neutron energy spectrum for $n(0.53 \text{ MeV}) + ^{235}\text{U}$ reaction in the laboratory frame. The experimental points are from Johansson and Holmqvist [20] at 0.53-MeV neutron energy.
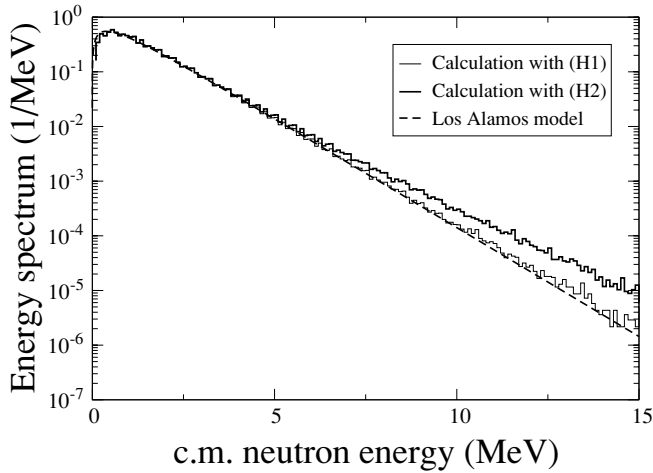
FIG. 6. Neutron energy spectrum in the FF center-of-mass system for ^{252}Cf(sf).

3. Level density parameter

In the present work, the level density parameter is defined as follows:

$$a(A, Z, U) = a^* \left\{ 1 + \frac{\delta W(A, Z)}{U} (1 - e^{-\gamma U}) \right\}. \qquad (16)$$

where $U = E^* - \Delta(A, Z)$, $\gamma = 0.05$, a^* is the asymptotic level density parameter [9]. The pairing Δ and shell correction δW energies for the FF were taken from the nuclear mass formula of Koura *et al.* [10]. The level density parameters a^* approximate to $A/7.25$ [11].

4. Total kinetic energy

The total kinetic energy is used to calculate the total FF excitation energy distribution. It is assumed to be approximately Gaussian in shape [see Eq. (7)] with an average value and width taken from the experimental data (Ref. [6] for the spontaneous fission of ^{252}Cf and Ref. [7] for the neutron induced
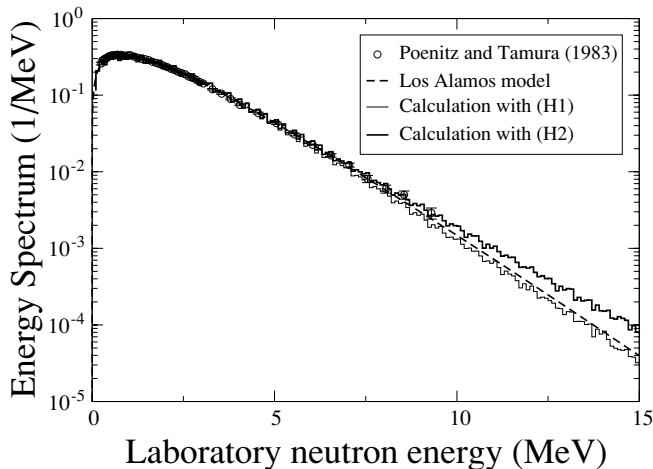

FIG. 7. Neutron energy spectrum for ^{252}Cf(sf) in the laboratory frame. The experimental points are from Poenitz and T. Tamura [22].
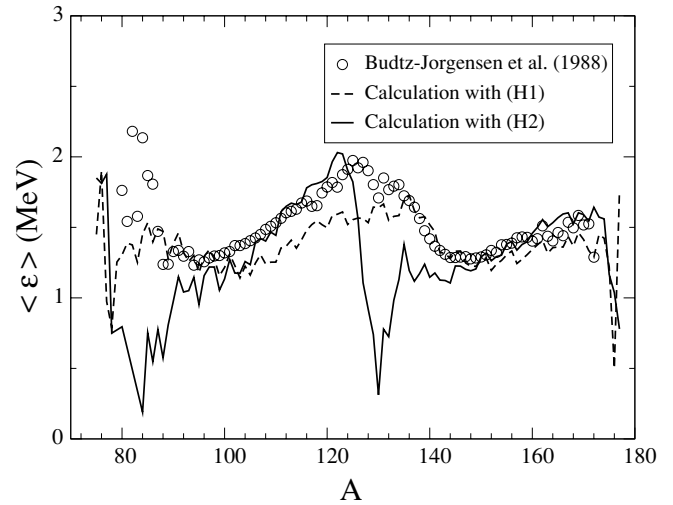

FIG. 8. Average neutron emission energy, $\langle \varepsilon \rangle$, in the center-of-mass frame as a function of FF mass for ^{252}Cf(sf). The points are experimental data from Ref. [12].

$n(0.53 \text{ MeV})+^{235}$U reaction). In our calculation, we take into account the fact that the total kinetic energy of a pair of FF can never exceed the energy released in the fission of Eq. (6) for the given pair, that is, we maintain energy conservation as much as possible (see Fig. 1).

5. Compound nucleus cross section

For sake of simplicity, we have assumed constant inverse reaction cross section in Eq. (12). This approximation will be lifted in our next works.

6. Average number of prompt fission neutrons $\bar{\nu}(A)$

We have used the average number of emitted neutrons $\bar{\nu}_{\exp}(A)$, the average neutron energy as a function of the FF, $\langle \varepsilon \rangle_{\exp}(A)$ and the total average γ-ray energy $\bar{E}_{\exp,\gamma}(A)$ as a way
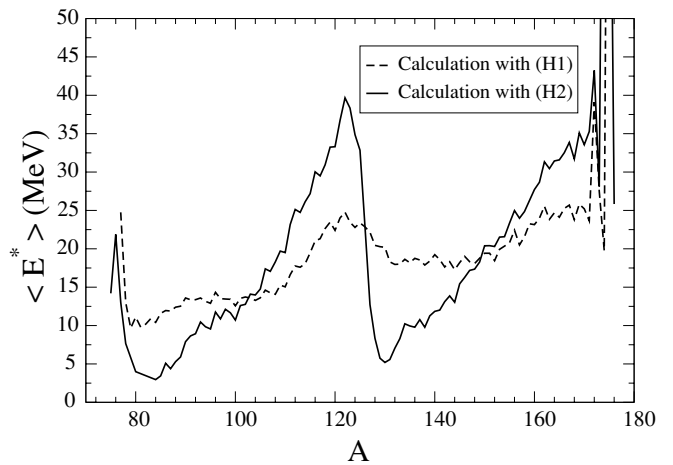

FIG. 9. Average initial fragment excitation energy as a function of FF mass number under both assumptions (H1) and (H2) for ^{252}Cf(sf).

TABLE I. Average prompt neutron multiplicities, initial excitation energies, and total γ-ray energies.

Fission reaction		$\bar{\nu}_L$	$\bar{\nu}_H$	$\bar{\nu}$	$\langle E^* \rangle_L$	$\langle E^* \rangle_H$	$\langle \bar{E}_\gamma \rangle_L$	$\langle \bar{E}_\gamma \rangle_H$
^{235}U$+n$(0.53 MeV)	H1	1.15	1.58	2.73	11.51	13.05	3.75	3.41
	H2	1.58	1.09	2.67	14.95	9.60	3.76	3.37
	Nishio et al. [13]	1.42	1.01	—				
	Diven et al. [15]	—	—	2.47				
^{252}Cf (sf)	H1	1.74	2.44	4.18	16.30	18.96	3.81	3.42
	H2	2.18	1.91	4.09	20.22	15.04	3.86	3.28
	Boldeman et al. [16]	—	—	3.7661				
	Vorobyev et al. [18]	2.05	1.70	3.76				

of partitioning the total excitation energy distribution between the light and heavy fragment. For the spontaneous fission of ^{252}Cf we used data from Ref. [12] on $\bar{\nu}_{\exp}(A)$ and $\langle \varepsilon \rangle_{\exp}(A)$. For the neutron induced n(0.53 MeV)$+^{235}$U reaction, we used data from Refs. [13,14] on $\bar{\nu}_{\exp}(A)$, $\langle \varepsilon \rangle_{\exp}(A)$, and $\bar{E}_{\exp,\gamma(A)}$.

III. RESULTS AND DISCUSSION

Our Monte Carlo simulations were done using 10^9 events for both spontaneous fission of ^{252}Cf and neutron induced n(0.53 MeV)$+^{235}$U reactions. Numerical results were obtained for various prompt fission neutron observables for the two energy partition hypotheses considered, (H1) and (H2). We checked that results obtained with the (H2) hypothesis, given by Eq. (9), are very similar to the one obtained using the approximation given in Eq. (11).

A. Prompt neutron multiplicity distribution

The prompt neutron multiplicity distribution $P(\nu)$ can be inferred from our MC calculations, whereas most other approaches can only assess the average value of this distribution, $\bar{\nu}$.
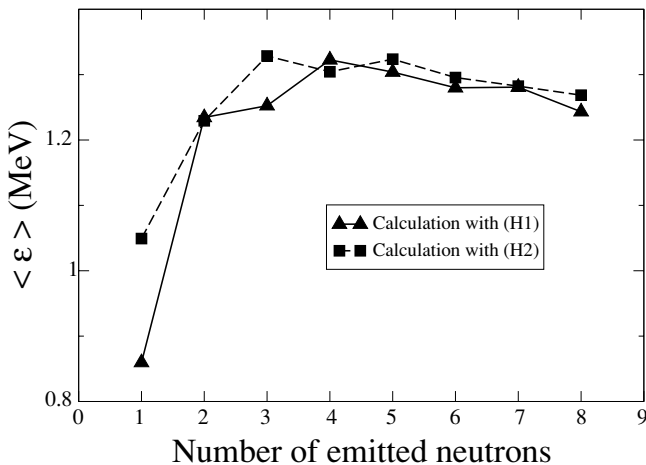
To the best of our knowledge, only a limited number of experimental data exist for $P(\nu)$. Our numerical results are compared with the experimental distribution by Diven et al. [15] in Fig. 2 for ^{235}U and with Terrell et al., Balagna et al., and Vorobyev et al. [17,18] for ^{252}Cf in Fig. 3. In both calculated cases (H1) and (H2), the average $\bar{\nu}$ of the distribution is larger than the experimental value. Average prompt neutron multiplicities for the light and heavy fragments are shown in Table I. Roughly speaking, the calculated $\bar{\nu}$ values are 10% higher than the experimental values. The dispersions of the calculated distributions are comparable to the experimental ones.

In the (H1) hypothesis of equal FF temperature at scission, the $\bar{\nu}$ value averaged over the heavy fragments yields is higher than the one for the light fragments, reflecting the higher average excitation energy available in the heavy fragments (cf. Table I). In the (H2) calculation, the initial excitation energy partitioning is constrained by experimental $\bar{\nu}_{\exp}$ values, thereby ensuring that the calculated ratio $\bar{\nu}_L/\bar{\nu}_H$ is very close to the experimental one.

We checked the sensitivity of our results on various parameters involved in the simulation. It appeared that the limit of the FF excitation energy beyond which no neutrons
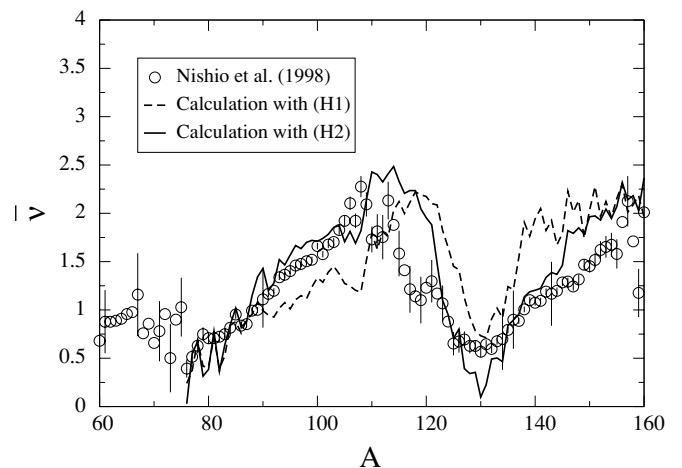

FIG. 10. Average center-of-mass neutron energies as a function of neutron multiplicity for the n(0.53 MeV)$+^{235}$U reaction.

FIG. 11. Average neutron multiplicity $\bar{\nu}$ as a function of the mass number of the FF for n(0.53 MeV)$+^{235}$U reaction. The points are experimental data from Ref. [13] at thermal incident neutron energy.
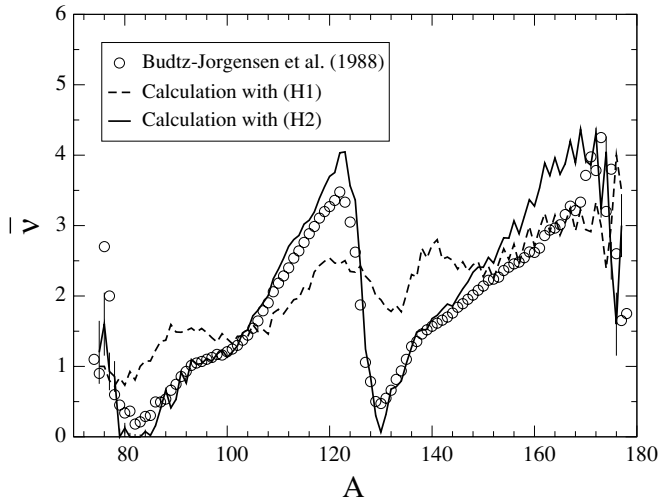
FIG. 12. Average neutron multiplicity $\bar{\nu}$ as a function of the mass number of the FF for ^{252}Cf(sf). The points are experimental data from Ref. [12].

are emitted is of great importance. In particular, choosing this limit to be equal to the neutron separation energy plus pairing energy rather than just the neutron separation energy leads to much better results on neutron energy spectra and neutron multiplicity distributions for both hypotheses of partitioning the available total excitation energy. This condition impacts our calculation by lowering neutron emission at excitation energy close to the neutron separation energy thus reflecting the increasing competition with γ-ray emissions.

B. Prompt fission neutron spectrum

For the neutron-induced reaction on ^{235}U, the neutron energy spectrum in the center of mass and laboratory frames are shown in Figs. 4 and 5 respectively. Also shown for
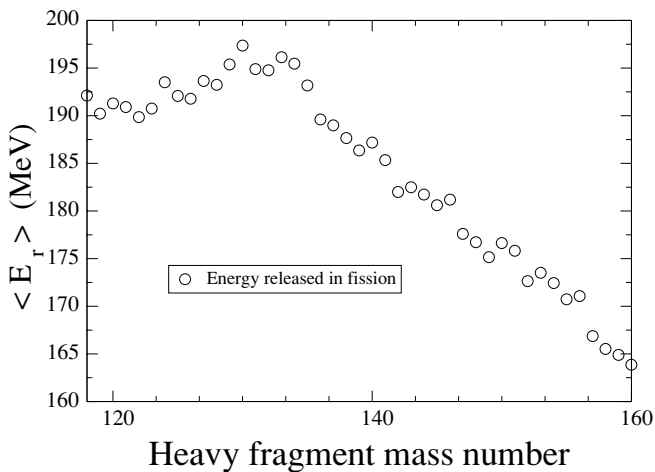

FIG. 13. Average energy released in fission as a function of the heavy fragment mass for the $n(0.53$ MeV)$+^{235}$U reaction, obtained from the difference between the compound nucleus and the FF masses given by the data table by Audi, Wapstra, and Thibault [8].
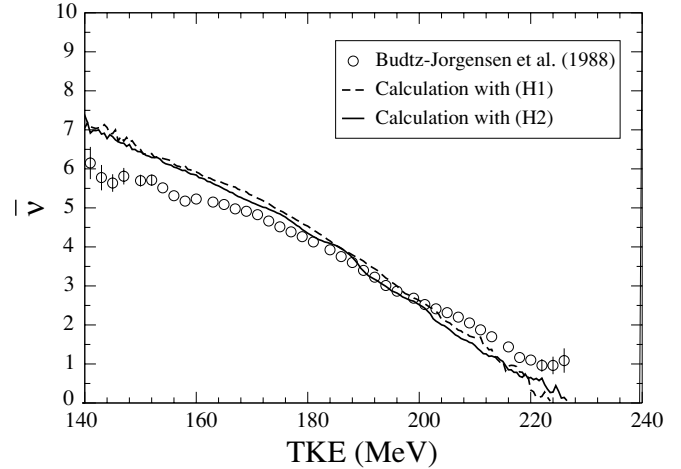

FIG. 14. Sum of the neutron multiplicities from both FF plotted as a function of TKE for ^{252}Cf(sf). The points are experimental data from Ref. [12].

comparison are the results obtained with the Los Alamos model for the same reaction using an optical model potential of Becchetti and Greenlees [19] for the average fragment of each peak. Experimental data points by Johansson and Holmqvist [20] are reported for the Laboratory spectrum. The calculated center-of-mass spectrum obtained by assuming equal nuclear temperatures in both FF at scission is shown to agree very well with the Los Alamos model calculation in Fig. 4, whereas the alternative hypothesis of splitting the energy according to $\bar{\nu}_{exp}(A)$ exhibits a much too hard spectrum. It is shown in Fig. 5 that none of our results manage to reproduce experimental data points by Johansson and Holmqvist [20] with a too-soft laboratory spectrum for the calculation made under (H1) assumption and a too-hard spectrum in the (H2) case.

As shown in Fig. 6 both center-of-mass spectra obtained under (H1) and (H2) hypotheses are too hard when compared
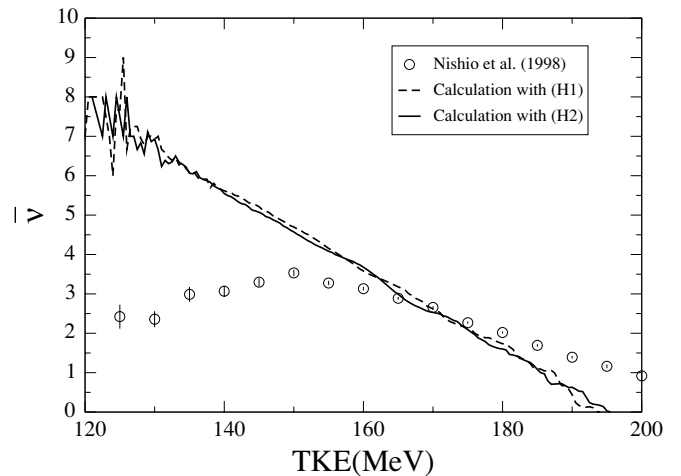

FIG. 15. Sum of the neutron multiplicities from both FF plotted as a function of TKE for $n(0.53$ MeV)$+^{235}$U reaction. The points are experimental data from Ref. [13] measured at thermal incident neutron energy.

TABLE II. Mean energies of prompt fission neutron spectra.

Fission reaction		Center-of-mass system			Laboratory system		
		$\langle \varepsilon \rangle_L$ (MeV)	$\langle \varepsilon \rangle_H$ (MeV)	$\langle \varepsilon \rangle$ (MeV)	$\langle E \rangle_L$ (MeV)	$\langle E \rangle_H$ (MeV)	$\langle E \rangle$ (MeV)
^{235}U+n(0.53 MeV)	H1	1.206	1.266	1.241	2.208	1.743	1.939
	H2	1.408	1.068	1.269	2.410	1.535	2.053
	Los Alamos model [1]	—	—	1.265	—	—	2.046
	Nishio *et al.* [13]	1.330	1.430	—	—	—	—
^{252}Cf (sf)	H1	1.335	1.393	1.368	2.273	1.934	2.074
	H2	1.542	1.223	1.392	2.468	1.743	2.128
	Los Alamos model [21]	—	—	1.366	—	—	2.134
	Poenitz and Tamura [22]	—	—	—	—	—	2.144

with the Los Alamos model for ^{252}Cf(sf) [21]. We point out that the calculation made under (H1) assumption seems to be in fairly good agreement with that of the Los Alamos model. The same degree of agreement, with experimental data points
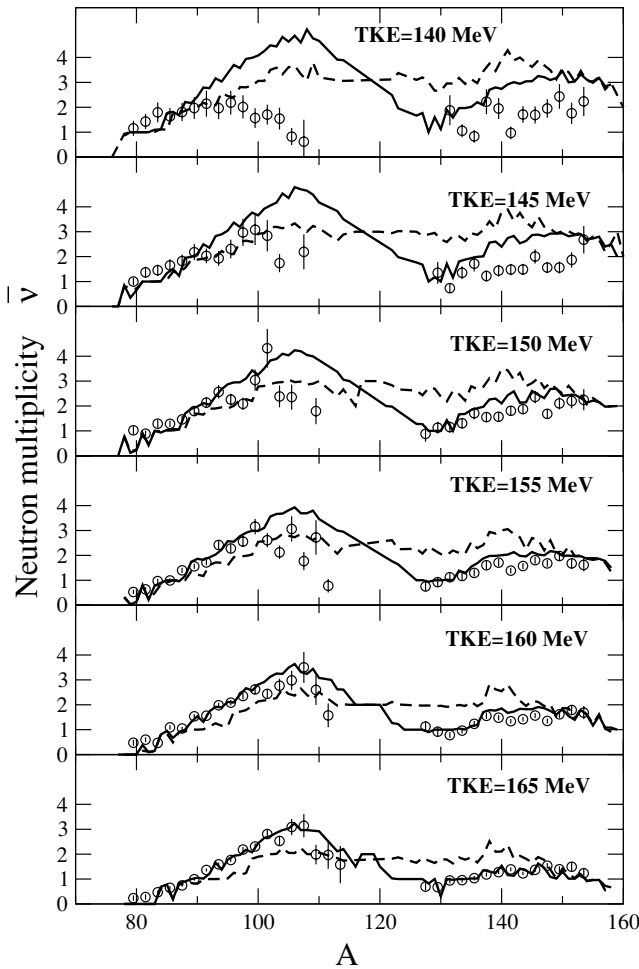

FIG. 16. Average neutron multiplicity versus FF mass for specific 5-MeV TKE bins for the n(0.53 MeV)+^{235}U reaction. The points are experimental data from Ref. [13] measured at thermal incident neutron energy. The dash and full lines are the results obtained under (H1) and (H2) hypotheses respectively.

by Poenitz and Tamura [22], is obtained for the laboratory neutron energy spectrum with the two assumptions made as we can see in Fig. 7.

It is interesting to note that the (H1) results agree very well for the center-of-mass neutron energy spectrum but disagree for the laboratory frame. In our calculation, the transformation from the center-of-mass to the laboratory frame is carried out exactly by taking into account the FF recoil energy after each neutron emission. Conversely, the Los Alamos model calculations assume an average recoil kinetic energy. For high-energy neutrons out, the exact recoil kinetic energy deviates significantly from this average kinetic energy and leads to discrepancies between the two results.

Note that our Monte Carlo simulations assume a constant inverse reaction cross section. It was shown in Ref. [1] that a more realistic Becchetti and Greenlees potential tends to lower the high-energy tail of the spectra. An energy-dependent reaction cross section may make the calculated spectra in Fig. 5 softer; accordingly, the calculated spectrum with (H2) hypothesis would be improved.

Calculated and experimental average neutron energy values are shown in Table II. It is observed experimentally that the average center-of-mass neutron energy emitted from the heavy fragment, $\langle \varepsilon \rangle_H$, is higher than the one emitted from the light fragment ($\langle \varepsilon \rangle_L$). This behavior is reproduced in the frame of the (H1) hypothesis but not within the (H2) hypothesis. For average laboratory neutron energies we obtained higher values for the light fragment than for the heavy one for both assumptions considered. This result is obtained for both studied reactions.

In addition to the calculated total neutron energy spectrum, we can investigate individual fragment spectra and extract from them an average center-of-mass neutron energy as a function of A. In Fig. 8, we compare the distribution of average neutron energies in the center-of-mass frame as a function of the FF mass number with experiments for ^{252}Cf(sf) [13]. The result obtained under the (H2) hypothesis agrees better with experimental data in the mass region $A_l \sim 105$–124 and $A_h \sim 145$–170. Large deviations appear in the mass region $A_l \sim 80$–105 and $A_h \sim 124$–144. To understand this behavior, we have to look at the inital excitation energy available in each fragment shown in Fig. 9. In particular, it is interesting to note that the regions where deviations appear correspond to
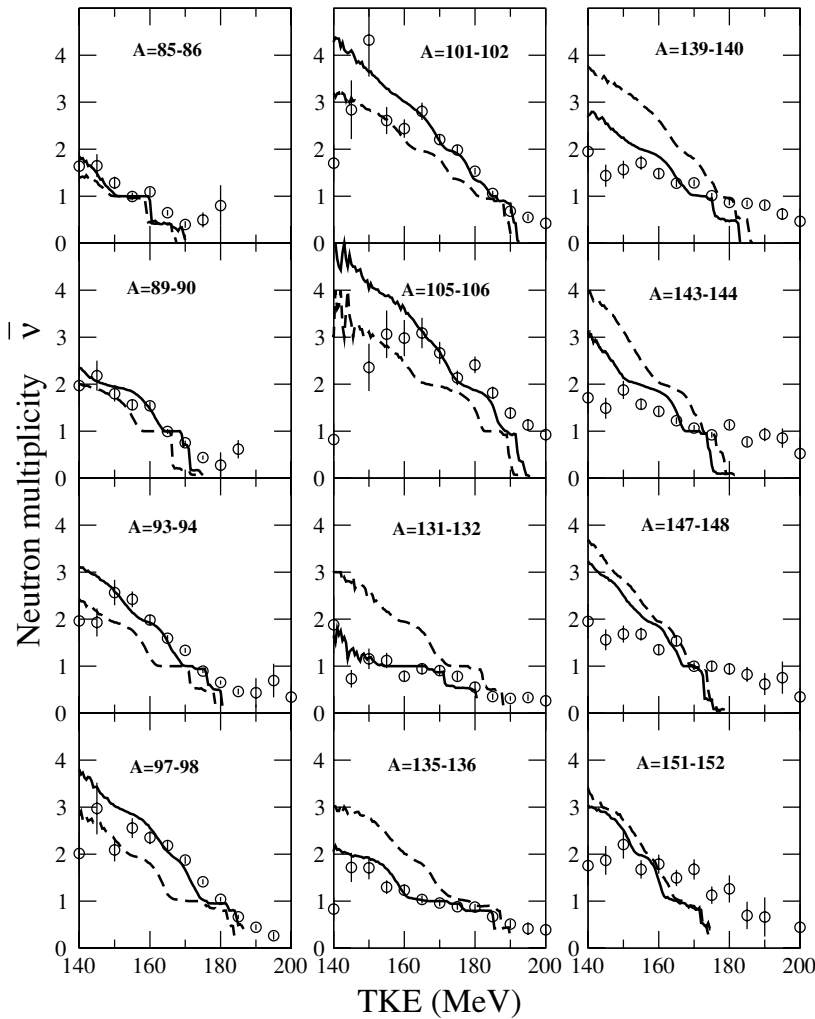
FIG. 17. Average neutron multiplicity plotted versus TKE for specified mass bins of width of 2 u for the $n(0.53$ MeV$)+^{235}$U reaction. The points are experimental data from Ref. [13] measured at thermal incident neutron energy. The dash and full lines are the results obtained under (H1) and (H2) hypotheses respectively.

fragments with excitation energies of the order of the neutron separation energy ($E^*_{l,h} \sim 5$–10 MeV) or less. As noted by Weisskopf in Ref. [5], in this case, the probability of emitting a neutron is less than that predicted by Eq. (14).

The result obtained under the (H1) hypothesis agrees with experimental data on the heavy fragment mass region $A \sim 135$–169 but fails in the light fragment mass region $A \sim 96$–135. The same conclusions, but less pronounced,

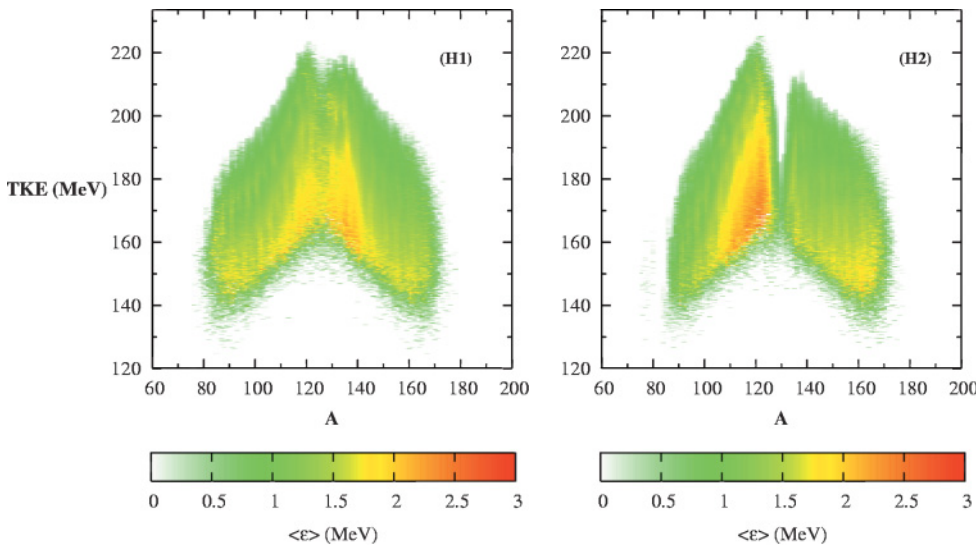

FIG. 18. (Color) Average center-of-mass neutron energy as a function of the mass number of the FF and TKE for ^{252}Cf(sf).
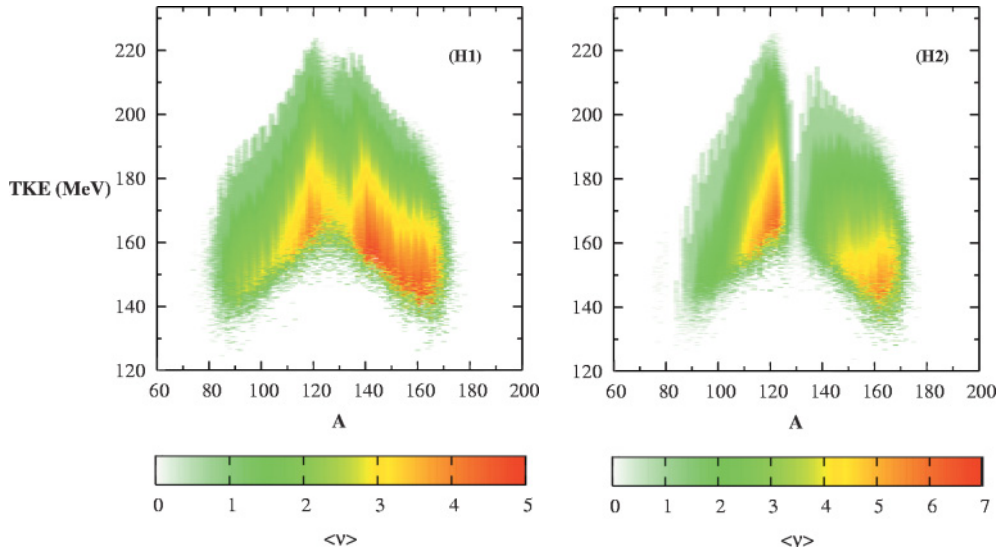
FIG. 19. (Color) Three-dimensional representation of the average neutron multiplicity $\bar{\nu}$ as a function of the mass number of the FF and TKE for ^{252}Cf(sf).

are drawn for the neutron-induced fission reaction on ^{235}U. A summary of the average initial FF excitation energies are given in Table I for the light and heavy fragment mass region for both assumptions.

Our calculation is based on a Fermi gas assumption $E^* = aT^2$. This leads to an overall too-high nuclear temperature for low FF excitation energies. An improvement would be to add a constant temperature region [23] to our description of neutron emission sequence for low FF excitation energies and keep the Fermi gas formulation for higher excitation energies. Finally, the cross section for the inverse process of compound nucleus formation will next include the neutron energy dependence.

To conclude the average center-of-mass neutron energies, $\langle \varepsilon \rangle$, as a function of neutron multiplicity is shown in Fig. 10. It is observed that $\langle \varepsilon \rangle$ when only one neutron is emitted departs significantly from the higher neutron multiplicity

FIG. 20. Average total energy, $\bar{E}_\gamma$, of γ-rays emitted as a function of FF mass for $n(0.53\ \mathrm{MeV}) + ^{235}$U reaction. The points are from F. Pleasonton *et al.* [14] for thermal-neutron induced fission of ^{235}U.

cases. When looking at one-neutron events we see that they are dominant when the excitation energy of a FF lies between approximately B_n and $2B_n$, therefore shifting the one-neutron energy spectrum to the lower values. This information could be used by experimentalists when performing neutron detector calibration.

C. Average neutron multiplicities

A well-known and important feature of prompt fission neutrons is the sawtooth shape of the average number of emitted neutrons per fission as a function of the fragment mass. Experimental and calculated $\bar{\nu}(A)$ distributions are shown in Figs. 11 and 12. In both reactions studied, we expect the results under the (H2) assumption to be in better agreement with experiment as compared to the (H1) results, simply because the (H2) calculations use $\bar{\nu}_{\exp}(A)$ as an input parameter to partition TXE. In the case of ^{235}U, the (H1) calculation reproduces qualitatively a sawtooth behavior. This result does not hold in the case of ^{252}Cf(sf). It is important to point out that the behavior of this distribution around the symmetric fission, for both reactions studied, is mostly because of the overall constant value of the energy released in the fission $\langle E_r \rangle$ as a function of A in Fig. 13 and the increasing value of the average total fragment kinetic energy $\overline{\mathrm{TKE}}$ as a function of the fragment mass. Also interesting, in the case of (H1) hypothesis, the increase of $\bar{\nu}(A)$ around the masses 130 to 140 is essentially because of the drop of the average neutron binding energy $\langle B_n(A) \rangle$ in this mass region, allowing more neutrons to be emitted because of the higher available excitation energy.

Another quantity of interest that has been measured for both reactions is the total average number of emitted neutrons as a function of the total kinetic energy. Our results are compared with experimental data in Fig. 14 for ^{252}Cf(sf) and Fig. 15 for ^{235}U Ref. [18,24,25]. The fact that in our approach the total

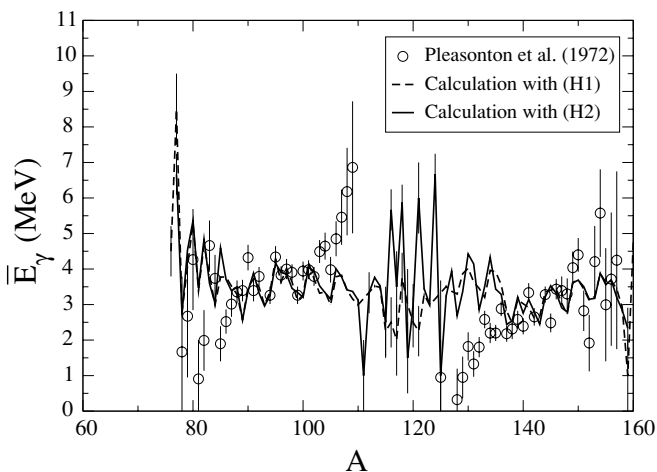excitation energy increase with decreasing TKE [see Eq. (5)] is responsible for the increase of $\bar{\nu}$(TKE). In addition, because the same total excitation energy TXE is available whatever the partitioning is, similar results are obtained for the calculated $\bar{\nu}$(TKE) under both (H1) and (H2) assumptions (Figs. 14 and 15).

Our calculations deviate from experimental results by overpredicting $\bar{\nu}$ for low TKE (below 164 MeV for ^{235}U reactions and below 168 MeV for ^{252}Cf). Some deviations also appear for higher TKE (above 179 MeV for ^{235}U reactions and above 203 MeV for ^{252}Cf) where we predict too few prompt neutrons as compared to experimental data. In the particular case of neutron-induced fission of ^{235}U a dramatic deviation between calculation and experiment on $\bar{\nu}$ is observed for low TKE that would indicate the presence of additional opened channels.

As pointed out earlier, the only knowledge of $\bar{\nu}$(TKE) cannot distinguish between the (H1) and (H2) hypotheses. However, one observable that would be sensitive to the partitioning of TXE is the distribution $\bar{\nu}(A, \text{TKE})$. Both measurements and calculations are compared in Figs. 16 and 17 for ^{235}U. Figure 16 shows some cuts of $\bar{\nu}(A)$ versus TKE (for the following specific total kinetic energies 140, 145, 150, 155, 160, and 165 MeV). To the best of our knowledge no similar measurements have been performed in the case of ^{252}Cf(sf). The comparison of our results with data in both Figs. 16 and 17 clearly show different behaviors under (H1) and (H2) assumptions. The (H2) calculation is in better agreement with experimental points. However, some deviations are observed for mass numbers $A \sim 101$–102 and $A \sim 105$–106 at low TKE (140, 145, and 150 MeV), reflecting the observation made earlier on $\bar{\nu}$(TKE). In the particular region of total kinetic energy peak (TKE $\sim$ 165 MeV), see Fig. 1, our calculation under the (H2) assumption is in fair agreement with experimental data (Figs. 16 and 17).

Figures 18 and 19 show our calculated $\bar{\nu}(A, \text{TKE})$ and $\langle \varepsilon \rangle (A, \text{TKE})$ for ^{252}Cf(sf) under both assumptions (H1) and (H2). These plots summarize most features discussed before.

D. Average total γ-ray energy

In our approach, the average total energy carried away by γ rays is obtained as the average excitation energy left when no further neutron emission is possible. Figure 20 compares calculated and experimental results for the reaction $n(0.53 \text{ MeV}) + ^{235}$U. Although the overall calculated energy $\overline{E}_\gamma$ averaged over all mass fragments A is in fair agreement with the experimental data, the experimental trend as a function of A is not correctly reproduced. A summary of averaged γ-ray energies is given in Table I. Our model will be improved in

future work to more precisely account for neutron and γ-ray emission competition.

IV. CONCLUSION

In conclusion, we have developed a new tool to explore the process of neutron evaporation from the statistical decay of fission fragments. The choice of a Monte Carlo implementation to describe this decay process allows us to infer important physical quantities that could not be assessed otherwise, for instance, within the Los Alamos model framework. In particular, the multiplicity distribution of prompt neutrons $P(\nu)$, the distribution of ν as functions of the FF mass number and total kinetic energy, and neutron-neutron correlations have all been inferred from the present Monte Carlo calculations.

This simulation tool can also be used to assess the validity of physical input assumptions, in particular the important question of how does the available total excitation energy get distributed among the light and heavy fission fragments.

The results reported in the present article shed some light on this question. By using the simple and natural assumption of equal nuclear temperatures in both light and heavy fragments at the scission point, average observables such as the average number of prompt fission neutrons $\bar{\nu}$ are fairly well reproduced by the calculation. However, more detailed physical quantities such as the distribution $\bar{\nu}(A, \text{TKE})$ show significant discrepancies between numerical and experimental values. To solve this problem, we have considered splitting the TXE between the two fragments by linking to experimental values for $\bar{\nu}(A)$ and $\langle \varepsilon \rangle (A)$. Under this assumption, the experimental distribution $\bar{\nu}(A, \text{TKE})$ is better reproduced, as expected. However, the calculated prompt neutron spectra are then not in good agreement with experiment any longer. Thus, neither (H1) nor (H2) are entirely adequate. So an (H3) option must be found.

Of interest is the distribution of the total number of prompt neutrons $\bar{\nu}$ as a function of TKE. At low TKE, experiments suggest a decrease of $\bar{\nu}$. In our approach, lower values of TKE correspond to higher values for TXE, which is then entirely dissipated by evaporating neutrons, followed by a γ-ray cascade. Therefore, higher values of TXE imply larger number of prompt neutrons emitted. To better reproduce the experimental values, it is necessary to treat properly the neutron-γ-ray competition. More work remains to be done to clarify this point.

[1] D. G. Madland and J. R. Nix, Nucl. Sci. Eng. **81**, 213 (1982).

[2] J. P. Unik *et al.*, in *Proceedings of the Third IAEA Symposium on Physics and Chemistry of Fission, Rochester, NY, 1973* (IAEA, Vienna, 1974), Vol. II, p. 19.

[3] W. Reisdorf, J. P. Unik, H. C. Griffin, and L. E. Glendenin, Nucl. Phys. **A177**, 337 (1971).

[4] J. C. Browne and F. S. Dietrich, Phys. Rev. C **10**, 2545 (1974).

[5] V. Weisskopf, Phys. Rev. **52**, 295 (1937).

[6] F. J. Hambsch and S. Oberstedt, Nucl. Phys. **A617**, 347 (1997).

[7] H. W. Schmitt, J. H. Neiler, and F. J. Walter, Phys. Rev. **141**, 1146 (1966).

[8] G. Audi, A. H. Wapstra, and C. Thibault, Nucl. Phys. **A729**, 337 (2003).

[9] A. V. Ignatyuk, K. K. Istekov, and G. N. Smirenkin, Sov. J. Nucl. Phys. **29**, 450 (1979).

[10] H. Koura, M. Uno and T. Tachibana, and M. Yamada, Nucl. Phys. **A674**, 47 (2000); H. Koura, T. Tachibana, M. Uno, and M. Yamada (private communication, 2004).

[11] T. Kawano (private communication, 2004).

[12] C. Budtz-Jørgensen and H. H. Knitter, Nucl. Phys. **A490**, 307 (1988).

[13] K. Nishio, Y. Nakagome, H. Yamamoto, and I. Kimura, Nucl. Phys. **A632**, 540 (1998).

[14] F. Pleasonton, R. L. Ferguson and H. W. Schmitt, Phys. Rev. C **6**, 1023 (1972).

[15] B. C. Diven, H. C. Martin, R. F. Taschek, and J. Terrell, Phys. Rev. **101**, 1012 (1956).

[16] J. W. Boldeman, in *Proceedings of the NEANDC Meeting on Nuclear Data Standards for Nuclear Measurements* (Uppsala University, Uppsala, Sweden, 1991), p. 108.

[17] J. P. Balagna, J. A. Farrell, G. P. Ford, A. Hemmendinger, D. C. Hoffmann, L. R. Vesser, and J. B. Wilhelmy, in *Proceedings of the Third International Atomic Energy Symposium on the Physics and Chemistry of fission, Rochester, 1973* (IAEA, Vienna, 1974), Vol. 2, p. 191.

[18] A. S. Vorobyev, V. N. Dushin, F. J. Hambsch, V. A. Jakovlev, V. A. Kalinin, A. B. Laptev, B. F. Petrov, and O. A. Shcherbakov, *Proceedings of the International Conference on Nuclear Data for Science & Technology*, ND2004, Santa Fe, Sep. 26–Oct. 1 (2004).

[19] F. D. Becchetti, Jr., and G. W. Greenlees, Phys. Rev. **182**, 1190 (1969).

[20] P. I. Johansson and B. Holmqvist, Nucl. Sci. Eng. **62**, 695 (1977).

[21] D. G. Madland and J. R. Nix, in *Proceedings of the NEANDC Specialists Meeting on Yields and Decay data of Fission Product Nuclides, Brookhaven National Laboratory, Long Island, NY, 1983* (BNL, 1974, report BNL51778 UC-34c), p. 423.

[22] W. P. Poenitz and T. Tamura, in *Proceedings of the International Conference on Nuclear Data for Science and Technology, Antwerp, Belgium, 1982* (Reidel Publishing, Dordrecht, Holland, 1983), p. 465 [the average energy results from a Maxwellian fit to the complete experimental spectrum].

[23] A. Gilbert and A. G. W. Cameron, Can. J. Phys. **43**, 1446 (1965).

[24] F. Gönnenwein, Pont d'Oye V, Seminar on fission, Pont d'Oye, 2003.

[25] V. Kalinin *et al.*, *Proceedings of the International Conference on Nuclear Data for Science & Technology*, ND2004, Santa Fe, Sep. 26–Oct. 1 (2004).